Letter Vol. 50, No. 19/1 October 2025/Optics Letters 6020

Optics Letters

200-km multi-user fully connected quantum entanglement distribution network in noisy environments

Yunlong Hou,[1,†] Yilin Yang,[2,†] Zhantong Qi,[2,†] Hao Li,[2] Yuanhua Li,[1,2,*] Jia Lin,[1,5] Yuanlin Zheng,[2,3] and Xianfeng Chen[2,3,4,6]

[1]Shanghai Key Laboratory of Materials Protection and Advanced Materials in Electric Power, Shanghai University of Electric Power, Shanghai 20090, China
[2]State Key Laboratory of Advanced Optical Communication Systems and Networks, School of Physics and Astronomy, Shanghai Jiao Tong University, Shanghai 200240, China
[3]Shanghai Research Center for Quantum Sciences, Shanghai 201315, China
[4]Collaborative Innovation Center of Light Manipulation and Applications, Shandong Normal University, Jinan 250358, China
[5]jlin@shiep.edu.cn
[6]xfchen@sjtu.edu.cn
[†]These authors contributed equally to this work.
*lyhua1984@shiep.edu.cn

Received 5 June 2025; revised 26 August 2025; accepted 27 August 2025; posted 28 August 2025; published 22 September 2025

Long-distance entanglement distribution is a fundamental operation for achieving a large-scale and scalable fully connected quantum communication network. However, current entanglement distribution methods cannot simultaneously meet the requirements of increasing user numbers and distribution distances. Here, we develop a three-user fully connected entangled distribution quantum network in the experiment. We demonstrate that the self-made periodically poled lithium niobate (PPLN) waveguide can achieve a fidelity of over 96% for the entangled state shared between users in the network. The results show that by introducing additional noise, the fidelity of the entangled state shared between any two users in the network is still greater than 85% after completing entanglement distribution over 200 km, which is far higher than the fidelity without adding noise. Our work provides a new, to the best of our knowledge, approach and experimental basis for building a large-scale and scalable fully connected quantum communication network over long distances.

https://doi.org/10.1364/OL.569922

Quantum entanglement distribution is a crucial approach for constructing large-scale, fully connected, scalable quantum communication networks. This technology is currently widely applied in various fields of quantum information processing, including quantum teleportation [1–4], quantum key distribution (QKD) [5–7], quantum repeaters [8,9], and quantum secure direct communication (QSDC) [10]. Moreover, it plays an essential role in the development of different types of quantum communication networks, such as QKD networks [11–13], quantum entanglement swapping networks [14,15], quantum entanglement distribution networks [16–18], QSDC networks [19,20], and fully connected multi-user quantum networks [21,22].

In a large-scale quantum communication network, we achieve long-distance quantum information processing tasks through quantum entanglement distribution [23]. However, as the complexity of the network and the number of users continue to increase, current entanglement distribution technologies struggle to maintain high fidelity and support long-distance quantum communication tasks. Advances in photonic-chip-based quantum networks [24–26] have also demonstrated significant progress toward scalable quantum communication. Recently, Huang *et al.* [27] developed a 16-user quantum communication network, but it can only perform QKD tasks between any two users up to 100 km apart, with no key sharing possible beyond 200 km. Fortunately, our preliminary research has found that, in noisy conditions, reducing the fidelity of the entangled state shared between users can enable long-distance quantum communication tasks [28], such as quantum secret sharing, quantum teleportation [29], and quantum entanglement distribution [30]. Therefore, by introducing additional noise, we can construct a scalable and fully connected long-distance quantum entanglement distribution network.

Here, we propose a long-distance multi-user fully connected quantum entanglement distribution network in noisy environments, utilizing M self-made periodically poled lithium niobate (PPLN) waveguide-integrated chips to achieve a large-scale fully connected quantum network for N users. In this work, we present a fully connected quantum entanglement distribution network spanning 200 km for three users by incorporating additional noise. We employ two bespoke micron-scale PPLN waveguides to create entangled photon pairs, subsequently dividing the generated single photons across six international telecommunication union (ITU) channels and allocating the

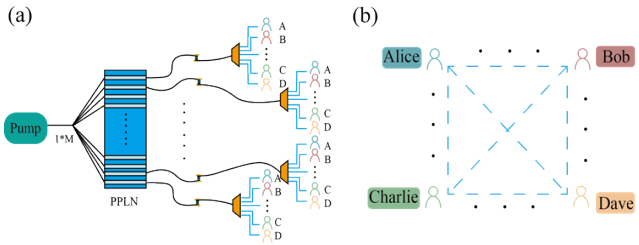

Fig. 1. Fully connected topologically long-distance quantum network with integrated PPLN waveguides.

time-energy entangled state to three users. The fidelity of the entangled state shared among users exceeds 96%. It is shown that the fidelity of the entangled state shared between any two users within the network remains above 85% after 200 km of entanglement distribution by modulating the amount of noise. This fidelity is considerably greater than that achieved without the addition of noise. Our experiment offers a novel solution for the development of a large-scale, scalable, fully connected, and long-distance quantum communication network.

We design a multi-user fully connected quantum network based on the integration of multiple PPLN waveguides. Integrating M PPLN waveguides on a single chip, when a pump light is injected into the M waveguides through a $1 \times M$ beam splitter (BS), the spectral width of the photon pairs generated via the spontaneous parametric down-conversion (SPDC) process in the PPLN waveguides has a full width at half maximum (FWHM) that exceeds 150 nm. As shown in Fig. 1, when the number of users in the network is N, we need at least $\frac{N(N-1)}{2}$ pairs of entangled photons to achieve a fully connected entanglement among all users, with each user operating at $N-1$ wavelengths. Since each PPLN waveguide can generate a maximum of 20 pairs of entangled photons in the C-band (1530–1565 nm), one PPLN waveguide can support the fully connected network of up to 6 users. As the number of users in the fully connected network increases, we can achieve their fully connected entanglement by increasing the number of PPLN waveguides. Here, we consider a simple case, using $M = 2$ PPLN waveguides to achieve a fully connected quantum network for $N = 3$ users. In our experiment, we use two temperature-stable type-0 PPLN micro-waveguides with a thickness of 3 μm and a length of 1.5 cm. With a cross-section of $3 \times 4\ \mu m^2$ and side walls angled at around 65 degrees.

Considering the noise model, in practical entanglement distribution scenarios, noise is inevitable. Here, we consider bit-flip noise. Bit-flip noise affects both channels. Assuming that each qubit is independently affected by the noise in the entanglement distribution process, the initial global density matrix can be described as follows [31]:

$$\varrho = \sum_{i=1}^{n_a} \sum_{j=1}^{n_b} E_{ij}(p_a, p_b)\, \rho E_{ij}^{\dagger}(p_a, p_b). \tag{1}$$

Here, $E_{ij}(p_a, p_b) = F_i(p_a) \otimes G_j(p_b)$, where $F_i(p_a) = F_i(p_a) \otimes 1$ and $G_j(p_b) = 1 \otimes G_j(p_b)$ represents Kraus operators associated with the noise types acting on one user and another user entangled qubits, respectively. n_a and n_b respectively represent the number of Kraus operators required to describe the noise in two channels. Since we are considering only two types of noise, F_i and G_j specifically denote the Kraus operators for bit-flip. Due to the possibility of different noises acting at different times, we explicitly show the dependence of the Kraus operators on these probabilities p_a and p_b. The p_a and p_b represent the extent of the noise impact on two channels, respectively. When we set $p_a = p_b = 0$, it corresponds to the noiseless case.

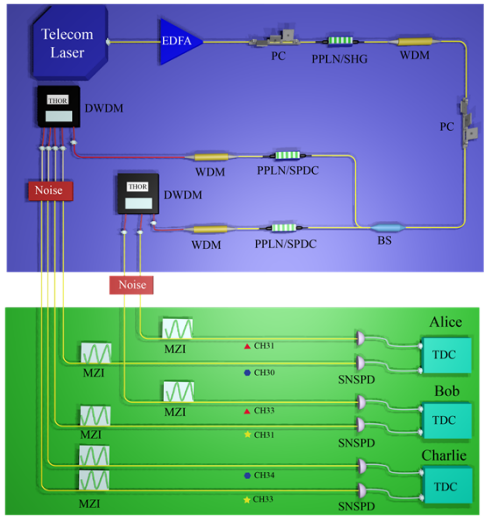

Fig. 2. Experimental setup. Multi-user fully connected quantum entanglement distribution network in noisy environments. PC, polarization controller; SNSPD, superconducting nanowire single-photon detector; TDC, time-to-digital converter.

The improvement of entanglement fidelity by adding bit-flip noise is caused by the noise compensation mechanism. Although noise usually reduces the fidelity of entangled states, our system utilizes controllable bit-flip noise to counteract the environmental noise accumulated during long-distance optical fiber transmission. The experimental setup is illustrated in Fig. 2. First, a continuous-wave laser at 1551.7 nm is amplified to 11 mW using an erbium-doped fiber amplifier (EDFA) and then used to excite the first PPLN waveguide for frequency doubling, generating a pump light with a central wavelength of 775.8 nm. To remove any residual 1551.7 nm laser light, we insert a wave division multiplexer (WDM) with 180 dB high isolation before the pump light enters the second PPLN for SPDC. Through these operations, we successfully obtain broadband SPDC photon pairs at the output of the second PPLN. Throughout this process, both the second harmonic generation (SHG) and SPDC fully utilize the quasi-phase-matching (QPM) properties of the PPLN, requiring the system temperature to be stably maintained at 325.4 K. Considering that single-photon detectors respond to 775.8 nm light as well, we again use a WDM to filter out this pump light and employ a DWDM with 100 GHz spacing to separate the generated photon pairs by wavelength. In the next step, we add a polarization controller (PC) into each user channel to intentionally introduce additional bit-flip noise. In our experiment, we systematically calibrate the azimuthal angles of the PC's three-paddle fiber loops while monitoring the single-photon detection rate in real time. When the detection rate reaches its maximum value, this indicates that the externally introduced bit-flip noise has reached an optimal level to compensate for the inherent bit-flip noise in the environment. Each end user is equipped with two 1 GHz unbalanced Mach-Zehnder interferometers (MZI) and two superconducting nanowire detectors. These detectors have efficiencies that exceed 80%, dark count rates below 40 counts per second, and

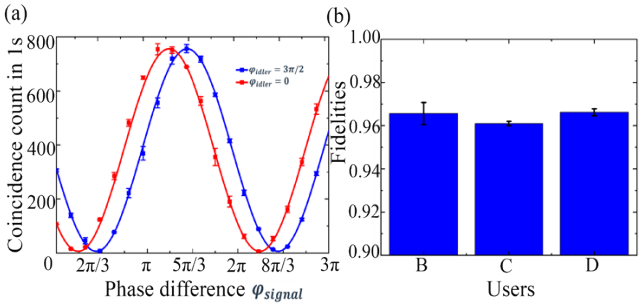

Fig. 3. (a) Two-photon interference fringes of Alice and Bob at 0 km. (b) Fidelity of entangled photon pairs between users at 0 km.

employ time-correlated single-photon counting technology to record detection events. The coincidence time window for the entire experiment is set to 500 picoseconds.

To achieve time-energy entangled photon pairs, we employ a Franson interferometer composed of an MZI. When the correlated photon pairs enter the MZI, if both photons travel along the same path, either the long arm or the short arm, the expression for the corresponding entangled state is:

$$|\psi_\theta\rangle = cos\,\theta|ss\rangle + sin\,\theta|ll\rangle, \tag{2}$$

where $|s\rangle$ and $|l\rangle$ respectively represent the quantum state of photons passing through the short and long paths of the MZI.

In the experiment, to ensure the capture of correlation effects between photon pairs while avoiding interference caused by single-photon coherence, the time parameters must satisfy the constraint $\tau_1 \gg \tau_3 > \tau_2$. Here, $\tau_1 = 1\,\mu s$ is the coherence time of the pump laser; $\tau_2 = 10\,ps$ is the coherence time of a single photon; and $\tau_3 = 1\,ns$ corresponds to the time delay introduced by the optical path difference between the two arms of the MZI. The relative phase difference between the MZI arms is actively controlled by applying voltage to resistive heaters.

In the experiment, the CH32 channel is selected from the C-band. The first waveguide generates CH30 and CH31 for connecting Alice and Bob, the second waveguide generates CH33 and CH31 for connecting Alice and Charlie, and CH34 and CH30 for connecting Bob and Charlie. Then, a multi-user fully connected quantum network is constructed. In this setup, continuous-wave pumping of PPLN waveguides generates time-energy entangled photon pairs through the SPDC process. Due to the spontaneous nature of the SPDC process, the generation time of each photon pair is random, leading to a corresponding relationship between the energies (i.e., frequencies) of the two photons, but the exact time at which each photon is generated remains uncertain. This temporal uncertainty results in a short coherence time for the photon pairs, meaning that their mutual correlations are limited in the time domain.

To measure the entanglement characteristics, we construct time-energy quantum networks. In the experiment, we set the phases of Bob MZI to 0 and $3\pi/2$, respectively. By changing the MZI voltage of Alice for phase scanning, the two-photon interference fringes can be obtained as shown in Fig. 3(a). We also measure two-photon interference fringes between other pairwise users. We estimated the maximum relevant fidelity based on $F = (1+3V)/4$ [32]. Where V is the interference visibility. The result shows the fidelity of $F_{AB}^{EXP} = (96 \pm 0.2)\%$, $F_{BC}^{EXP} = (96 \pm 0.4)\%$, and $F_{AC}^{EXP} = (96 \pm 0.4)\%$, which are presented in Fig. 3(b).

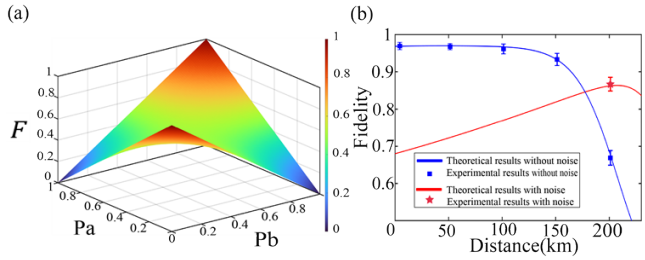

Fig. 4. (a) Change in entanglement fidelity when both Alice and Bob are affected by bit-flip noise. (b) Relationship between fidelity and distance, with and without noise.

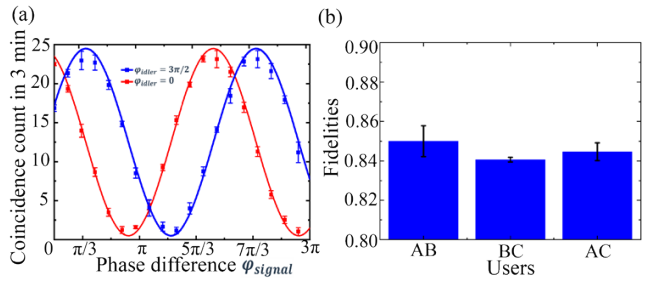

Fig. 5. (a) Two-photon interference fringes of Alice and Bob at 200 km. (b) Fidelity of entangled photon pairs between users at 200 km.

The fidelity in quantum networks can be effectively improved by adjusting the channel noise. We consider that both Alice and Bob are subject to bit-flip noise. The fidelity of entanglement can be given by:

$$F(\theta) = (1-p_a)(1-p_b) + p_a p_b sin^2 2\theta\,. \tag{3}$$

Here, $F(\theta)$ denotes the entanglement fidelity. p_a and p_b represent the extent of the noise impact on Alice's and Bob's channels, respectively.

From Eq. (3), when in the maximum entangled state, we can draw the picture about the variation of F with p_a and p_b as shown in Fig. 4(a). We can find that the fidelity F decreases at the beginning as p_a and p_b increases. Furthermore, when p_a and p_b are greater than 0.5, the fidelity F will increase. Theoretically, the fidelity of entanglement can reach 1.

Without the introduction of additional noise, we can obtain the blue curve of fidelity with distance according to the theory, and the experimental results are consistent with the theory [33], as shown in Fig. 4(b). We find that the entanglement fidelity is lower than the classical fidelity thresholds [34,35] of 2/3 after 200 km transmission.

In the case of extra noise, we add bit-flip noise to the two channels, Alice and Bob, and the entanglement fidelity will be improved compared with the case without noise. This shows that the quantum network still maintains good entanglement characteristics after 200 km transmission. It can be seen that even with artificially added bit-flip noise, it is still impossible to achieve a theoretical fidelity of 1. When the transmission distance exceeds 200 km, the fidelity curve declines. Beyond 200 km, inherent limitations like fiber loss and dispersion dominate, inevitably degrading fidelity.

Considering the noise and the distance of 200 km, we measure the two-photon interference curves of Alice and Bob as shown in Fig. 5(a), and we can obtain the fidelity of FAB

$F_{AB}^{EXP} = (85 \pm 0.7)\%$. The error bars in Fig. 5(a) represent the standard deviation of repeated measurements ($N = 3$ trials) under identical conditions. In the same way, we obtain the fidelities between the other two users $F_{BC}^{EXP} = (84 \pm 0.1)\%$, $F_{AC}^{EXP} = (84 \pm 0.4)\%$, as shown in Fig. 5(b).

In the future, we can use pump light at a specific frequency, based on a single integrated chip with M PPLN waveguides of identical performance, to generate entangled photon pairs that can be used to achieve a large-scale entanglement fully connected network for N users.

In summary, we successfully achieved a 200-km multi-user fully connected quantum entanglement distribution network in noisy environments by utilizing two PPLN waveguides and DWDM technology. Through the PPLN waveguides, we generated three pairs of entangled photons and distributed them to three users to construct the network. This network provided a time-energy entangled state with a fidelity greater than 96% to facilitate entanglement distribution tasks among the three users. Furthermore, bit-flip affects both channels. We demonstrated that, under optimized noise parameters, the fidelity of the entangled photon pairs could still reach 85% after transmission over 200 km, significantly surpassing scenarios without added noise. Our approach paves a new way for constructing an efficient and robust quantum communication network under complex real-world conditions.

Funding. National Natural Science Foundation of China (12074155, 62375164, 12192252); Shanghai Municipal Science and Technology Major Project (2019SHZDZX01-ZX06); Shuguang Program of Shanghai Education Development Foundation and Shanghai Municipal Education Commission (24SG53); Guangdong Provincial Quantum Science Strategic Initiative (GDZX2403003).

Disclosures. The authors declare no conflicts of interest.

Data availability. Data underlying the results presented in this paper are not publicly available at this time but may be obtained from the authors upon reasonable request.

REFERENCES

1. J. G. Ren, P. Xu, H. L. Yong, *et al.*, Nature **549**, 70 (2017).
2. J. Wang, S. Paesani, Y. Ding, *et al.*, Science **360**, 285 (2018).
3. J. Zhao, H. Jeng, L. O. Conlon, *et al.*, Nat. Commun. **14**, 4745 (2023).
4. F. Basso Basset, F. Salusti, L. Schweickert, *et al.*, NPJ Quantum Inf. **7**, 7 (2021).
5. V. Scarani, H. Bechmann-Pasquinucci, N. J. Cerf, *et al.*, Rev. Mod. Phys. **81**, 1301 (2009).
6. F. Xu, X. Ma, Q. Zhang, *et al.*, Rev. Mod. Phys. **92**, 025002 (2020).
7. S. Utagi, R. Srikanth, and S. Banerjee, Process **19**, 366 (2020).
8. Z. D. Li, R. Zhang, X. F. Yin, *et al.*, Nat. Photon. **13**, 644 (2019).
9. J. Dias, M. S. Winnel, N. Hosseinidehaj, *et al.*, Phys. Rev. A **102**, 052425 (2020).
10. Y. B. Sheng, L. Zhou, and G. L. Long, Sci. Bull. **67**, 367 (2022).
11. M. Mehic, M. Niemiec, S. Rass, *et al.*, ACM Comput. Surv. **53**, 96 (2020).
12. M. Sasaki, M. Fujiwara, H. Ishizuka, *et al.*, Opt. Exp. **19**, 10387 (2011).
13. C. X. Huang, X. M. Hu, B. H. Liu, *et al.*, Sci. Bull. **67**, 593 (2022).
14. G. Guccione, T. Darras, H. Le Jeannic, *et al.*, Sci. Adv. **6**, eaba4508 (2020).
15. Y. Li, Y. Huang, T. Xiang, *et al.*, Phys. Rev. Lett. **123**, 250505 (2019).
16. K. Chakraborty, D. Elkouss, B. Rijsman, *et al.*, IEEE Trans. Quantum Eng. **1**, 4101321 (2020).
17. X. Yang, Y. H. Yang, and M. X. Luo, Phys. Rev. Res. **4**, 013153 (2022).
18. Y. Cao, Y. Zhao, Q. Wang, *et al.*, IEEE Commun. Surv. Tuts. **24**, 839 (2022).
19. Z. Qi, Y. Li, Y. Huang, *et al.*, Light Sci. App. **10**, 183 (2021).
20. D. Pan, X. T. Song, and G. L. Long, Adv. Devices Instrum. **4**, 0004 (2023).
21. S. Wengerowsky, S. K. Joshi, F. Steinlechner, *et al.*, Nature **564**, 225 (2018).
22. X. Liu, J. Liu, R. Xue, *et al.*, PhotoniX **3**, 2 (2022).
23. D. Aktas, B. Fedrici, F. Kaiser, *et al.*, Laser Photon. Rev. **10**, 451 (2016).
24. Y. Zheng, C. Zhai, D. Liu, *et al.*, Science **381**, 221 (2023).
25. L. T. Feng, M. Zhang, D. Liu, *et al.*, Phys. Rev. Lett. **135**, 020802 (2025).
26. D. Liu, Z. Jin, J. Liu, *et al.*, Light Sci. Appl. **14**, 243 (2025).
27. Y. Huang, Z. Qi, Y. Yang, *et al.*, Laser Photon. Rev. **19**, 2301026 (2025).
28. R. Fortes and G. Rigolin, Phys. Rev. A **92**, 012338 (2015).
29. Z. D. Liu, O. Siltanen, T. Kuusela, *et al.*, Sci. Adv. **10**, eadj3435 (2024).
30. S. Ecker, F. Bouchard, L. Bulla, *et al.*, Phys. Rev. X **9**, 041042 (2019).
31. R. Fortes and G. Rigolin, Phys. Rev. A **93**, 062330 (2016).
32. H. de Riedmatten, I. Marcikic, J. A. W. Van Houwelingen, *et al.*, Phys. Rev. A **71**, 050302 (2005).
33. T. Honjo, H. Takesue, H. Kamada, *et al.*, Opt. Exp. **15**, 13957 (2007).
34. J. F. Clauser, M. A. Horne, A. Shimony, *et al.*, Phys. Rev. Lett. **23**, 880 (1969).
35. I. Marcikic, H. De Riedmatten, W. Tittel, *et al.*, Phys. Rev. Lett. **93**, 180502 (2004).